JOURNAL OF COMPUTATIONAL PHYSICS **134,** 96–107 (1997)
ARTICLE NO. CP975675

Discrete Transparent Boundary Conditions for Schrödinger-Type Equations

Frank Schmidt* and David Yevick†

*Konrad-Zuse-Zentrum für Informationstechnik Berlin, D-14195 Berlin-Dahlem, Germany; †Queen's University, Department of Electrical Engineering, Kingston, Ontario, Canada K7L 3N6
E-mail: Frank.Schmidt@zib.de

Received May 28, 1996; revised February 10, 1997

We present a general technique for constructing nonlocal transparent boundary conditions for one-dimensional Schrödinger-type equations. Our method supplies boundary conditions for the θ-family of implicit one-step discretizations of Schrödinger's equation in time. The use of Mikusiński's operator approach in time avoids direct and inverse transforms between time and frequency domains and thus implements the boundary conditions in a direct manner.

1. INTRODUCTION

This paper is concerned with the construction of transparent boundary conditions for evolution partial differential equations of the type

$$\partial_t u = -\frac{i}{c}(\partial_x^2 u + V(x,t)u), \quad x \in \mathbf{R}, t > 0, \qquad (1)$$

$$u(x,0) = u_0(x).$$

Here c is a real constant and $V(x,t)$ denotes the potential to be specified later. Prototypes of this equation are the Schrödinger equation for an electron with mass m_0,

$$i\hbar\partial_t\Psi = -\frac{\hbar^2}{2m_0}\partial_x^2\Psi + V(x,t)\Psi,$$

and Fresnel's equation for the evolution of a paraxial electrical field E along the z-direction in a Cartesian coordinate system,

$$2in_0k_0\partial_z E = \partial_x^2 E + (n^2(x) - n_0^2)\,k_0^2 E.$$

The evolution equation (1) is defined in the infinite domain $\Omega = \{x, t \in \mathbf{R} | t > 0\}$, where the physical boundary conditions are imposed. For example, if $u_0(x)$ has support only in a finite interval and $\|u_0(x)\|_{L^2}$ is bounded, we expect that $u(x, t)$ must vanish if $x \to \pm\infty$ at any time $t > 0$. For practical purposes, however, the required computational effort is limited by the fact that we wish to compute the solution of (1) only in a finite subdomain of Ω in order to examine the time evolution in the surrounding of a specified object. In our 1D-case, we accordingly separate the infinite domain Ω into three slab-like parts: an interior domain of finite thickness $\Omega_i = \{x, t \in \mathbf{R} \mid x_l \le x \le x_r, t > 0\}$ containing the physically relevant part of the solution and two neighboring slabs of infinite thickness $\Omega_l = \{x, t \in \mathbf{R} \mid x \le x_l, t > 0\}$ and $\Omega_r = \{x, t \in \mathbf{R} \mid x \ge x_r, t > 0\}$. The general question is then how to transform the zero-boundary conditions at infinity to the boundary conditions at the boundaries of the interior domain.

There are a large number of methods for constructing such boundary conditions, a few of which are discussed below. The methods can be grouped into two classes:

Artificially Absorbing Layers. One set of simple but powerful boundary conditions continuously modify the potential functions in the exterior domain in order to simulate a physical absorber. The parameters have to be adjusted such that backward diffraction from the absorber is small over a prescribed spectral range, c.f. [7], [14], [8], [13]. The main advantage of such an approach, as has been remarked by a large number of authors, is its simplicity for two and three-dimensional problems.

Approximate Solutions in the Entire Physical Domain. A second class of methods is obtained by analytically constructing boundary conditions in such a manner that the solutions in the interior domain approximate as accurately as possible the whole-space solution of the evolution equation. Following the pioneering work of Engquist and Majda [4] on hyperbolic equations, a number of approximation techniques have been proposed for mixed parabolic-hyperbolic systems (Halpern [5]) or parabolic equations (Hagstrom [6]). In these papers, by Laplace transforming in time, the partial differential equation is converted to a second-order ordinary differential equation, which is then solved allowing only for decaying modes in

0021-9991/97 $25.00

the exterior domains. After transforming into the time-domain the resulting transparent boundary conditions in general become nonlocal in time but are local in space. Computationally advantageous approximations that require little additional computational effort are then obtained by applying a rational approximation to the dispersion relation in the dual frequency domain.

However, for problems in which minimizing the magnitude of the reflected field is more important than computational cost, nonlocal boundary conditions are generally advantageous. The two main categories of nonlocal conditions are, first, methods in which the continuous problem is solved first and then discretized with respect to time, as suggested by Baskakov and Popov [2]. However, such approaches may lead to numerical instabilities. In [9] Mayfield analyzed the stability of such a discrete scheme uniform in time (with time-step Δt) and space (with space-step Δx) and found that stability is given only in disjoined intervals for $\Delta t/\Delta x^2$. Alternatively, the analytical problem can be consistently formulated for discrete time. In this manner, Arnold [1] compose a boundary condition which incorporates both a uniform space and a uniform time discretization. In the direction of the space-coordinate his approach is exactly the same as the one of Eisenberg *et al.* [3], who used this continuation of the uniform discretized space coordinate to infinity to solve the time-independent 1D Schrödinger equation. In contrast, the approach by Schmidt and Deuflhard [11] supposes a given, possibly nonuniform, time-discretization and solves the related exterior ordinary differential equations in the spatial domain with the aid of the Laplace transform. We will label this approach the semi-discrete method. The advantage of the latter procedure is that the exterior space problem is solved exactly and independently of the solution method for the inner problem. Accordingly, the formalism may be easily extended to nonuniform interior discretizations and adaptive methods. On the other hand, Arnold's technique should generally be advantageous in simulations of wave propagations on uniform grids since reflections due to space-discretization effects are fully eliminated.

In this paper we demonstrate that the semi-discrete approach can encompass a uniform time-discretization in a consistent fashion, generating a simple, yet highly accurate transparent boundary condition. This boundary condition can be applied to all space-discretizations of the interior domain, which permit the specification of arbitrary Neumann conditions. Thus even pseudo-spectral methods [12] can be used to discretize the inner problem. Further we show that this approach may similarly be extended to a uniform space-discretization of the exterior domain and thus to the full discrete case. Our procedure employs both Laplace and Z-transforms in the space variable (and not in time) and the Mikusiński representation [10] of the time-discrete problem. We can accordingly construct the desired boundary conditions directly without transforming from the dual to the original domain.

In our analysis, we assume the following two properties of the domain decomposition and the potential function

- u_0 is supported in Ω_i
- $V(x, t) = \text{const}$ for $(x, t) \in \Omega_l$ and for $(x, t) \in \Omega_r$.

While the first of these conditions is not required, it significantly simplifies the analysis by allowing us to assume the asymptotic behavior $u(x, t) \to 0$ if $x \to \pm\infty$ for any time $t > 0$. The second condition, which can in fact be replaced by the weaker form $V(x, t) = V(t)$ as in [11], is realized by many practical problems and thus has similarly been chosen to permit a compact solution. Further, we assume $\mathcal{I}(V/c) \le 0$ to ensure the stability of the solution. Let us rewrite (1) as

$$\partial_t u = f(u, t), (x, t) \in \Omega$$

with

$$u(x, 0) = u_0(x)$$
$$\lim_{x \to \pm\infty} u(x, t) = 0.$$

To solve this equation numerically, we apply the implicit one-step discretization method

$$u_{i+1} - u_i = \tau f(\theta u_{i+1} + (1 - \theta)u_i, t_i + \theta\tau)$$
$$\tau = t_{i+1} - t_i, \quad i = 0, 1, ...,$$
$$0 < \theta \le 1.$$

It is known that for homogeneous Dirichlet boundary conditions this scheme is stable if $\frac{1}{2} \le \theta \le 1$. Using the definition of $f(u, t)$ from (1), we obtain

$$u_{i+1} - u_i = -i\frac{\tau}{c}((\partial_x^2 + V)(\theta u_{i+1} + (1 - \theta)u_i)). \quad (2)$$

The notation above will be particularly useful in our later implementation and stability analysis of the transparent boundary conditions in Sections 3.3 and 3.4. However, for constructing transparent boundary conditions, the following sequence of ordinary differential equations resulting from the time-discretization of the underlying partial differential equation, is more convenient:

$$\partial_x^2 u_{i+1} - \lambda^2 u_{i+1} = -\Theta\partial_x^2 u_i + \kappa^2 u_i$$
$$\Theta = \frac{1 - \theta}{\theta}$$
$$\lambda^2(x, t_i + \theta\tau) = \frac{ic}{\tau\theta} - V(x, t_i + \theta\tau) \quad (3)$$
$$\kappa^2(x, t_i + \theta\tau) = -\frac{ic}{\tau\theta} - \Theta V(x, t_i + \theta\tau).$$

We now seek solutions u_i, $i \geq 1$, of (3) that vanish at infinity. While we will eventually employ a discretization such as a finite-difference or finite-element representation to solve the interior problem, we focus here on obtaining an exterior solution which enables the boundary conditions to be constructed. For this purpose, we fix the right boundary at $x_r = 0$, $t > 0$ and search for solutions $u_i(x)$, $i \geq 1$, $x \geq 0$ in the right exterior domain. These exterior solutions have to obey the boundary condition at infinity

$$\lim_{x \to \infty} u_i(x) = 0, \quad i \geq 1. \tag{4}$$

2. PRELIMINARY CONSIDERATION

We first consider the solution, $u_1(x)$, of Eq. (1) in the exterior domain, $x \geq 0$, at the initial time step. This solution is obtained by solving

$$\partial_x^2 u_1 - \lambda^2 u_1 = 0,$$

which yields

$$u_1(x) = c_1 \exp(\lambda x) + c_2 \exp(-\lambda x),$$

where $\lambda = \sqrt{\lambda^2}$, $\Re(\lambda) > 0$. To satisfy the zero-boundary-condition at infinity (4), the values of $u_1(0)$ and $\partial_x u_1|_0$ must ensure that $c_1 = 0$, leading to the desired form of the solution:

$$u_1(x) = u_1(0) \exp(-\lambda x). \tag{5}$$

This yields the required transformation of the boundary conditions at infinity to the boundary condition at x_r for the first time step. By induction, representing each $u_i(x)$ by a convolution of the homogeneous part of the solution of (3) with the right-hand side of (3) and choosing the free constants as before such that $u_i(x)$ remains bounded for $x \to \infty$ we derive that the exterior solution at step i can be written as

$$u_i(x) = P_{i-1}(x) \exp(-\lambda x), \tag{6}$$

where $P_{i-1}(x)$ denotes a polynomial in x of degree $i - 1$. Alternatively, the exterior solution u_i can be obtained by regarding the Laplace transform

$$U_i(p) = \mathscr{L} u_i(x) = \int_0^\infty \mathrm{e}^{-px} u_i(x)\, dx.$$

Since the Laplace transform of each term in (6) follows from

$$\mathscr{L}\left\{\frac{x^n}{n!} \mathrm{e}^{-\lambda x}\right\} = \frac{1}{(p + \lambda)^{(n+1)}},$$

$U_i(p)$ is an analytic function on $\Re(p) > 0$ and satisfies

$$U_i(p) < \infty \quad \text{for all } p \text{ with } \Re(p) > 0. \tag{7}$$

Condition (7) may be regarded as an implicit formulation of the boundary condition (4) i.e., we have to choose the boundary conditions in such a way that (7) holds for any $i \geq 1$. Thus, in order to verify the condition for any time-step, we must analyze the sequence $U_1(p)$, ..., $U_{i+1}(p)$ (where the index here refers to the propagation step number) of Laplace-transformed solutions in the exterior domain. The recurrence relation for this sequence is given directly by the Laplace transformation of (3); namely,

$$U_{i+1} = \frac{pu_{i+1}(0) + \partial_x u_{i+1}|_{x=0} + \Theta(pu_i(0) + \partial_x u_i|_{x=0}) - (\Theta p^2 - \kappa^2) U_i}{p^2 - \lambda^2}. \tag{8}$$

To verify the condition (7), we investigate the poles of $U_{i+1}(p)$ in the right half-plane. We express each $U_i(p)$ as quotient of two polynomials. Since $U_1(p)$, given according to (5) by

$$U_1(p) = \frac{u_1(0)}{p + \lambda},$$

has the form $U_1(p) = P_1(p)/Q_1(p)$, we may assume that each $U_i(p)$ possesses the same structure, that is,

$$U_i(p) = \frac{P_i(p)}{Q_i(p)}, \quad P_i(p), Q_i(p)\text{-polynomials}.$$

From (8) we then obtain

$$U_{i+1}(p) = \frac{\tilde{P}_{i+1}(p)}{(p^2 - \lambda^2) Q_i}, \tag{9}$$

where $\tilde{P}_{i+1}(p)$ is an as yet undetermined polynomial. However, the above expression is in general unbounded for $p = \lambda$ and $\Re(\lambda) > 0$. Thus the related solutions u_{i+1} will diverge for $x \to \pm\infty$.

We therefore arrive at the central issue of the paper, namely the specification of appropriate boundary conditions which ensure the finiteness of $U_{i+1}(p = \lambda)$ for bounded $U_i(p)$ in the right half-plane. That is, we wish to

combine $u_{i+1}(0)$ and $\partial_x u_{i+1}|_0$ in $\tilde{P}_{i+1}(p)$, in such a manner that

$$\tilde{P}_{i+1}(\lambda) = 0. \tag{10}$$

As can easily be verified, the two free coefficients associated with the boundary value and the normal derivative can be combined in such a manner that the result factors as

$$\tilde{P}_{i+1}(p) = (p - \lambda) P_{i+1}(p).$$

This leads to a rational expression for $U_{i+1}(p)$ given by

$$\begin{aligned} U_{i+1}(p) &= \frac{(p-\lambda)P_{i+1}(p)}{(p-\lambda)(p+\lambda)Q_i(p)} \\ &= \frac{P_{i+1}(p)}{Q_{i+1}(p)}, \end{aligned}$$

and, therefore, to a polynomial Q_{i+1}, which does not contain zeros in the right half-plane if such zeros are absent in Q_i. Hence the solution $u_{i+1}(x)$ corresponding to Q_{i+1} possesses the required asymptotic behavior.

3. OPERATOR FORMULATION

We now formalize the above approach in such a manner that the desired boundary condition is automatically satisfied at each propagation step. As the method is based on the recursive strategy discussed above, it leads to a compact numerical procedure.

3.1. *Reformulation Using the Shift-Operator Technique*

We first introduce the shift-operator $s = \exp(-p_\tau \tau)$ with $p_\tau = \partial/\partial t$. In our notation this operator shifts the time index i by one unit

$$u_i(x) = s u_{i+1}(x).$$

Accordingly, by the linearity of the Laplace-transform,

$$U_i(p) = s U_{i+1}(p). \tag{11}$$

The technique of manipulating the shift-operator directly in real space without transforming the underlying equation into the dual, frequency, domain, is in accordance with the algebraic operator theory of Mikusiński [10]. According to this theory the shift-operator s can be manipulated as if it were a complex number. We present a simplified version of the Mikusiński formalism in the Appendix. We rewrite (8) and (9) as

$$U_{i+1}(p) = \frac{p u_{i+1}(0) + \partial_x u_{i+1}|_0 + \Theta(p u_i(0) + \partial_x u_i|_0)}{p^2 - \lambda^2 + s(\Theta p^2 - \kappa^2)}. \tag{12}$$

Evidently if the denominator of (12) approaches zero, i.e., if the semi-discrete dispersion relation

$$p^2 - \lambda^2 + s(\Theta p^2 - \kappa^2) = 0$$

is fulfilled, the homogeneous solution diverges at infinity unless the numerator simultaneously vanishes. The zeros of p occur at the solutions, $p = p_\pm$, of

$$p^2 = \frac{\lambda^2 + \kappa^2 s}{1 + \Theta s}, \tag{13}$$

which yields

$$p_\pm = \pm\lambda\sqrt{(1 + \kappa^2/\lambda^2 s)/(1 + \Theta s)}, \quad \Re(\lambda) > 0.$$

Therefore, the necessary condition that guarantees the exact solution of (3) is

$$p_+ u_{i+1}(0) + \partial_x u_{i+1}|_{x=0} + \Theta(p_+ u_i(0) + \partial_x u_i|_{x=0}) = 0, \quad i \geq 0. \tag{14}$$

The recursive structure of (14) combined with the requirement that $u_0(x) = 0$ for $x \geq 0$, yields finally the following compact form of the desired transparent boundary condition

$$p_+ u_{i+1}(0) + \partial_x u_{i+1}|_{x=0} = 0 \tag{15}$$

$$p_+ = \lambda\sqrt{(1 + \kappa^2/\lambda^2 s)/(1 + \Theta s)}, \quad \Re(\lambda) > 0. \tag{16}$$

For future implementation it is convenient to split p into a s-independent part and a second expression which has the property that each term in its Taylor series representation is homogeneous with respect to s according to

$$\begin{aligned} p_+ &= p_I + p_H \\ p_I &= \lambda \\ p_H(s) &= \lambda(-1 + \sqrt{(1 + \kappa^2/\lambda^2 s)/(1 + \Theta s)}). \end{aligned}$$

This representation enables us to separate the term corresponding to multiplication by a constant coefficient from terms that generate the index-shifts.

Special Case I: Implicit Midpoint Discretization. We now illustrate (15) for potential functions that vanish outside the inner domain Ω_i. Considering first an implicit midpoint discretization for which $\theta = 0.5$ and $\Theta = 1$, we have

$$p_+ = \lambda\sqrt{(1-s)/(1+s)} = \lambda(1 - s + \tfrac{1}{2}s^2 - \tfrac{1}{2}s^3 + \tfrac{3}{8}s^4 - \tfrac{3}{8}s^5 + \cdots), \quad (7)$$

yielding the boundary condition

$$\lambda u_{i+1} + \partial_x u_{i+1}|_{x=0} = \lambda(u_i - \tfrac{1}{2}u_{i-1} + \tfrac{1}{2}u_{i-2} - \tfrac{3}{8}u_{i-3} + \tfrac{3}{8}u_{i-4} - \cdots)|_{x=0}. \quad (18)$$

Special Case II: Implicit Euler Discretization. Considering next the implicit Euler scheme in the propagation direction, we apply instead $\theta = 1$ and $\Theta = 0$. We then obtain in place of Eqs. (17) and (18)

$$p_+ = \lambda\sqrt{1-s} = \lambda(1 - \tfrac{1}{2}s - \tfrac{1}{8}s^2 - \tfrac{1}{16}s^3 - \tfrac{5}{128}s^4 - \cdots),$$

and

$$\lambda u_{i+1} + \partial_x u_{i+1}|_{x=0} = \lambda(\tfrac{1}{2}u_i + \tfrac{1}{8}u_{i-1} + \tfrac{1}{16}u_{i-2} + \tfrac{5}{128}u_{i-3} + \cdots)|_{x=0}.$$

3.2. *Finite-Difference Implementation*

Having developed the continuous formulation of our transparent boundary condition, we now examine finite-difference and finite-element implementations. Considering first the finite-difference formalism, we wish to transform (3) into its corresponding discrete approximation. That is, we must replace $\partial_x^2 u$ by its discrete analogue on both the right- and the left-hand sides of (3). In the case of a uniform computational grid with a step-width $x^i - x^{i-1} = h$ for all inner points we substitute in standard fashion

$$\partial_x^2 u|_{x=x^i} \to \frac{1}{h^2}(u^{i-1} - 2u^i + u^{i+1})$$

with a $O(h^2)$ discretization error. At the $x = 0$ boundary, however, we instead apply the Taylor expansion of $u(x)$ at $x = 0$,

$$u(h) = u(0) + u'(0)h + \tfrac{1}{2}u''(0)h^2 + O(h^3),$$

to rewrite $\partial_x^2 u$ as

$$\partial_x^2 u|_{x=0} = \frac{2}{h^2}(u(-h) - u(0) + h\partial_x u|_{x=0}) + O(h).$$

Here we assume that $u(0)$, $u'(0)$ and the rightmost inner value $u(-h)$ are given. Thus we must rewrite the differential equation, (3), at the boundary in the finite-difference implementation as

$$(\partial_x^2 u + \text{const}\, u)_{x=0} \to \frac{2}{h^2}(u(-h) - u(0) + h\partial_x u|_{x=0}) + \text{const}\, u(0).$$

The above boundary condition is now substituted for the normal derivative of u, leading to the finite-difference representation of the transparent boundary condition.

3.3. *Finite-Element Implementation*

Next, we derive and discuss a transparent boundary condition analogous to that of the previous section, but based on a finite-element discretization of (2). The finite-element method automatically satisfies the symmetry properties required for numerical stability. However, many other discretization methods such as the finite-difference approach can be shown to possess identical symmetries and are therefore equally stable. The weak form of (2) is

$$(v, u_{i+1}) + i\frac{\tau}{c}\theta(\partial_x u_{i+1}|_{x=x_1}^{x=x_r} + a(v, u_{i+1})) = (v, u_i) + i\frac{\tau}{c}(1-\theta)(\partial_x u_i|_{x=x_1}^{x=x_r} - a(v, u_i)), \quad (19)$$

with

$$a(v,u) = -\int \partial_x \bar{v}\,\partial_x u + \int \bar{v}V(x)u \quad (20)$$

$$(v,u) = \int \bar{v}u \quad (21)$$

for any $v \in H^1(\Omega_i)$. Discretizing the problem restricts the test-function space to $V_h \subset H^1(\Omega_i)$. Accordingly, we obtain the matrices $\mathbf{A}$ and $\mathbf{M}$ from the bilinear forms $a(\cdot,\cdot) \to \mathbf{A}$ and $m(\cdot,\cdot) \to \mathbf{M}$. Hence the discrete version of (19) yields

$$\left(\mathbf{M} + i\frac{\tau}{c}\theta\mathbf{A}\right)\mathbf{u}_{i+1} + i\frac{\tau}{c}\theta\begin{pmatrix} -\partial_x u_{i+1}|_{x=x_1} \\ \mathbf{0} \\ \partial_x u_{i+1}|_{x=x_r}\end{pmatrix} = \left(\mathbf{M} - i\frac{\tau}{c}(1-\theta)\mathbf{A}\right)\mathbf{u}_i - i\frac{\tau}{c}(1-\theta)\begin{pmatrix} -\partial_x u_i|_{x=x_1} \\ \mathbf{0} \\ \partial_x u_i|_{x=x_r}\end{pmatrix}.$$

Together with the boundary condition (15), we arrive at the final form of the equation system

$$\left(\mathbf{M}+i\frac{\tau}{c}\theta\mathbf{A}\right)\mathbf{u}_{i+1}-i\frac{\tau}{c}\theta p_I\begin{pmatrix}u_{i+1}(x_\mathrm{l})\\ \mathbf{0}\\ u_{i+1}(x_\mathrm{r})\end{pmatrix}=\left(\mathbf{M}-i\frac{\tau}{c}(1-\theta)\mathbf{A}\right)\mathbf{u}_i$$

$$+i\frac{\tau}{c}(1-\theta)(p_+(s))\begin{pmatrix}u_i(x_\mathrm{l})\\ \mathbf{0}\\ u_i(x_\mathrm{r})\end{pmatrix}+i\frac{\tau}{c}\theta p_H(s)\begin{pmatrix}u_{i+1}(x_\mathrm{l})\\ \mathbf{0}\\ u_{i+1}(x_\mathrm{r})\end{pmatrix}. \tag{22}$$

3.4. *Stability Properties*

We now introduce the notation

$$\langle\mathbf{v},\mathbf{u}\rangle=\bar{\mathbf{v}}^{\mathrm{T}}\mathbf{u},$$

for Euclidean inner product, while the discrete L^2-product in terms of the symmetric positive definite matrix $\mathbf{M}$ defined above is written as

$$\langle\mathbf{v},\mathbf{u}\rangle_{\mathbf{M}}=\bar{\mathbf{v}}^{\mathrm{T}}\mathbf{M}\mathbf{u},$$

and the related discrete L^2-norm is

$$\|\mathbf{u}\|=\sqrt{\langle\mathbf{u},\mathbf{u}\rangle_{\mathbf{M}}}.$$

We now show that given matrix $\mathbf{A}$ which is self-adjoint with respect to the Euclidean inner product, for $0.5\le\theta\le 1$ the discrete $L^2(\Omega_\mathrm{i})$ norms of $\mathbf{u}_1$, ..., $\mathbf{u}_{i+1}$ obtained using (22) remain bounded for any time step τ. Hence our numerical scheme is unconditionally stable under these conditions. To prove our assertion, we again invoke the weak form of (2) that forms the basis of (22). We now, however, rearrange the expression as

$$(v,u_{i+1}-u_i)=-i\frac{\tau}{c}a(v,u_\theta)-i\frac{\tau}{c}((\bar{v}\partial_x u_\theta)|_{x=x_1}^{x=x_\mathrm{r}}) \tag{23}$$

with

$$u_\theta=\theta u_{i+1}+(1-\theta)u_i.$$

Restricting (23) again to its discrete form, setting $v=u_\theta$, and taking the real part yields

$$\Re\langle\mathbf{u}_\theta,\mathbf{u}_{i+1}-\mathbf{u}_i\rangle_{\mathbf{M}}=-\frac{\tau}{c}\Re(i(\bar{u}_\theta\partial_x u_\theta)|_{x=x_1}^{x=x_\mathrm{r}}).$$

A rearrangement of the terms in the above expression leads to

$$\langle\mathbf{u}_{i+1},\mathbf{u}_{i+1}\rangle_{\mathbf{M}}-\langle\mathbf{u}_i,\mathbf{u}_i\rangle_{\mathbf{M}}=-2(\theta-\tfrac{1}{2})$$
$$\langle\mathbf{u}_{i+1}-\mathbf{u}_i,\mathbf{u}_{i+1}-\mathbf{u}_i\rangle_{\mathbf{M}}-2\frac{\tau}{c}\Re(i(\bar{u}_\theta\partial_x u_\theta)|_{x=x_1}^{x=x_\mathrm{r}}).$$

The same procedure can be applied to the exact solutions of (2) in the exterior regions. For the right exterior domain $x\ge x_\mathrm{r}$

$$(u_{i+1},u_{i+1})-(u_i,u_i)=-2(\theta-\tfrac{1}{2})$$
$$(u_{i+1}-u_i,u_{i+1}-u_i)-2\frac{\tau}{c}\Re(i(\bar{u}_\theta\partial_x u_\theta)|_{x=x_\mathrm{r}}^{x=\infty})$$

with an analogous result for the left exterior domain. Our boundary conditions, however, preserve the exponential decay of the exact solution of (2) in the exterior domains as both exterior solutions are described by (6), with $\Re(\lambda)>0$. Hence, the boundary terms vanish as $x\to\infty$ and further cancel at $x=x_{\mathrm{l,r}}$ so that

$$\sum_{j=\mathrm{l,r}}(u_{i+1},u_{i+1})_{\Omega_j}+\langle\mathbf{u}_{i+1},\mathbf{u}_{i+1}\rangle_{\mathbf{M}}-\left(\sum_{j=l,r}(u_i,u_i)_{\Omega_j}+\langle\mathbf{u}_i,\mathbf{u}_i\rangle_{\mathbf{M}}\right)$$
$$=-2\left(\theta-\frac{1}{2}\right)\left(\sum_{j=\mathrm{l,r}}(u_{i+1}-u_i,u_{i+1}-u_i)_{\Omega_j}\right.$$
$$\left.+\langle\mathbf{u_{i+1}}-\mathbf{u_i},\mathbf{u_{i+1}}-\mathbf{u_i}\rangle_{\mathbf{M}}\right).$$

The right-hand side of the above expression is nonpositive for $\theta\ge 0.5$, establishing both the numerical stability of the algorithm and the uniqueness of the interior solution. Furthermore, for the implicit midpoint rule, $\theta=0.5$, we find

$$\sum_{j=\mathrm{l,r}}(u_i,u_i)_{\Omega_j}+\langle\mathbf{u}_i,\mathbf{u}_i\rangle_{\mathbf{M}}=\text{const}\quad\text{for all } i\ge 0. \tag{24}$$

Equation (24) extends the conservation property of the implicit midpoint rule with homogeneous Dirichlet or Neumann boundary conditions to the entire real space.

4. DISCRETE SOLUTION OF THE EXTERIOR PROBLEM

We now consider the case of uniform spatial discretization in the interior domain Ω_i. Under the assumption of a uniform grid point spacing in the exterior domain, an identical finite-difference stencil can be applied in both the interior and exterior domains, providing an approximate solution of the continuous problem. Hence in this particular case, completely reflection-free boundary conditions can be realized by sacrificing the quality of the approximation applied to the exterior domain. In contrast, the semi-discrete approach discussed above supplies the exact solu-

tion of (3) in the exterior domain, at the cost of a small residual reflection, which of course vanishes as $h \to 0$. The nature of the residual reflection is evident from a backward analysis of the problem in which the discrete inner solution is considered as the exact solution of a slightly modified equation. Unless the same discrete approximation is employed in the exterior and interior domains, the difference in the underlying equation in the two domains necessarily produces a small reflected field.

4.1. *Discrete Treatment of the Space Coordinate*

To implement the above procedure, we associate the solution points at the ith propagation step with physical locations according to the formula

$$u_i^{(j)} = u_i(j \cdot h), \quad j \geq -1, i \geq 0.$$

Here $u_i^{(-1)}$ is the rightmost inner value in Ω_i while u_i^0 is located on the boundary between the internal and the right external region. The equation corresponding to (12) is obtained by introducing the sequences

$$\begin{aligned} \mathrm{u}_i &= \{u_i^{(0)}, u_i^{(1)}, u_i^{(2)}, \ldots\} \\ \mathrm{u}_i^+ &= \{u_i^{(1)}, u_i^{(2)}, u_i^{(3)}, \ldots\} \\ \mathrm{u}_i^- &= \{u_i^{(-1)}, u_i^{(0)}, u_i^{(1)}, \ldots\}, \end{aligned}$$

with Z-transforms

$$\begin{aligned} \mathscr{U}_i &= \mathscr{Z}\mathrm{u}_i = u_i^{(0)} + \frac{1}{z} u_i^{(1)} + \frac{1}{z^2} u_i^{(2)} + \cdots \\ \mathscr{U}_i^+ &= \mathscr{Z}\mathrm{u}_i^+ = u_i^{(1)} + \frac{1}{z} u_i^{(2)} + \frac{1}{z^2} u_i^{(3)} + \cdots \\ \mathscr{U}_i^- &= \mathscr{Z}\mathrm{u}_i^- = u_i^{(-1)} + \frac{1}{z} u_i^{(0)} + \frac{1}{z^2} u_i^{(1)} + \cdots. \end{aligned}$$

Suppressing the time-step subscript i in the following, we observe next that the transforms $\mathscr{U}^+$ and $\mathscr{U}^-$ are related to $\mathscr{U}$ by

$$\mathscr{U}^- = \frac{1}{z}\mathscr{U} + u^{(-1)} \tag{25}$$

$$\mathscr{U}^+ = z(\mathscr{U} - u^{(0)}). \tag{26}$$

If we now Z-transform the finite-difference form of (3) in Ω_r,

$$\frac{1}{h^2}(u_{i+1}^{j-1} - 2u_{i+1}^j + u_{i+1}^{j+1}) - \lambda^2 u_{i+1}^j = -\frac{\Theta}{h^2}(u_i^{j-1} - 2u_i^j + u_i^{j+1}) + \kappa^2 u_i^j, \quad j \geq -1, i \geq 0,$$

we obtain

$$\frac{1}{h^2}(\mathscr{U}_{i+1}^- - 2\mathscr{U}_{i+1} + \mathscr{U}_{i+1}^+) - \lambda^2 \mathscr{U}_{i+1} = -\frac{\Theta}{h^2}(\mathscr{U}_i^- - 2\mathscr{U}_i + \mathscr{U}_i^+) + \kappa^2 \mathscr{U}_i, \quad i \geq 0.$$

This equation yields, in view of (25) and the shift-operator definition (11),

$$\mathscr{U}_{i+1}(z) = -\frac{u_{i+1}^{(-1)} - z u_{i+1}^{(0)} + \Theta(u_i^{(-1)} - z u_i^{(0)})}{z - (2 + h^2\lambda^2) + 1/z + s\Theta(z - (2 + h^2\kappa^2/\Theta) + 1/z)}.$$

Again in analogy to the continuous case, we now compute the zeros $z_\pm$ of the discrete dispersion relation

$$z - (2 + h^2\lambda^2) + \frac{1}{z} + s\Theta\left(z - \left(2 + h^2\frac{\kappa^2}{\Theta}\right) + \frac{1}{z}\right) = 0, \tag{27}$$

which are given by

$$z_\pm(s) = 1 + q_\pm(s) \tag{28}$$

with

$$\begin{aligned} q_\pm(s) &= c_1 \frac{1 + \beta^2 s}{1 + \Theta s} \pm c_2 \sqrt{\frac{1 + \beta^2 s}{1 + \Theta s}} \sqrt{\frac{1 + \gamma^2 s}{1 + \Theta s}} \\ c_1 &= \tfrac{1}{2} h^2\lambda^2 \\ c_2 &= \tfrac{1}{2}\sqrt{h^2\lambda^2}\sqrt{4 + h^2\lambda^2} \\ \gamma^2 &= \frac{4\Theta + h^2\kappa^2}{4 + h^2\lambda^2} \\ \beta^2 &= \frac{\kappa^2}{\lambda^2}. \end{aligned} \tag{29}$$

Applying the root-theorem of Vieta to (27) we find $z_+ z_- = 1$. If we define z_+ and z_- such that $|z_-| < 1$ and $|z_+| > 1$. Then, choosing the square roots such that $\Re(c_2) > 0$, the desired discrete counterpart to the transparent boundary condition (15) is given by

$$u_{i+1}^{(-1)} - z_+ u_{i+1}^{(0)} = 0,$$

or equivalently,

$$u_{i+1}^{(0)} - u_{i+1}^{(-1)} + q_+ u_{i+1}^{(0)} = 0. \tag{30}$$

4.2. *Implementation*

To incorporate (30) into a numerical code, we proceed exactly as in Section 3.3. In particular, we first derive the equation system for homogeneous Neumann conditions. We set formally $q_+ = 0$ to obtain the equation system

$$\left(\mathbf{M} + i\frac{\tau}{c}\theta\mathbf{A}\right)\mathbf{u}_{i+1} = \left(\mathbf{M} - i\frac{\tau}{c}(1-\theta)\mathbf{A}\right)\mathbf{u}_i, \quad (31)$$

after applying the FD-stencil to all inner points and discretizing the second derivative operator according to

$$\partial_x^2 u|_{x=x_r} \to \frac{1}{h^2}(u^{-1} - u^0)$$

for the right boundary with an analogous expression at the left boundary. Completing this system by imposing the boundary condition (30) yields

$$\left(\mathbf{M} + i\frac{\tau}{c}\theta\mathbf{A}\right)\mathbf{u}_{i+1} - i\frac{\tau}{ch^2}\theta q_+(s)\begin{pmatrix} u_{i+1}(x_l) \\ \mathbf{0} \\ u_{i+1}(x_r)\end{pmatrix}$$

$$= \left(\mathbf{M} - i\frac{\tau}{c}(1-\theta)\mathbf{A}\right)\mathbf{u}_i + i\frac{\tau}{ch^2}(1-\theta)_{q^+}(s)\begin{pmatrix} u_i(x_l) \\ \mathbf{0} \\ u_i(x_r)\end{pmatrix}.$$

After the operator q is separated into its homogeneous and inhomogeneous parts, we finally arrive at

$$\left(\mathbf{M} + i\frac{\tau}{c}\theta\mathbf{A}\right)\mathbf{u}_{i+1} - i\frac{\tau}{ch^2}\theta q_I\begin{pmatrix} u_{i+1}(x_l) \\ \mathbf{0} \\ u_{i+1}(x_r)\end{pmatrix} = \left(\mathbf{M} - i\frac{\tau}{c}(1-\theta)\mathbf{A}\right)\mathbf{u}_i$$

$$+ i\frac{\tau}{ch^2}(1-\theta)q_+(s)\begin{pmatrix} u_i(x_l) \\ \mathbf{0} \\ u_i(x_r)\end{pmatrix} + i\frac{\tau}{ch^2}\theta q_H(s)\begin{pmatrix} u_{i+1}(x_l) \\ \mathbf{0} \\ u_{i+1}(\mathbf{x}_r)\end{pmatrix}.$$

Numerical Stability. As the arguments presented in Section 3.4 are equally valid for the discrete problem, our implicit one-step methods are unconditionally stable for $0.5 \le \theta \le 1$, provided the discretization insures that matrix $\mathbf{M}$ is symmetric positive definite and that the matrix $\mathbf{A}$ is self-adjoint with respect to the Euclidean inner product.

5. APPLICATION TO THE FRESNEL EQUATION

Having outlined both the theory and the implementation of the discrete transparent boundary conditions we now investigate the two test cases of [14] associated with optical beam propagation in the Fresnel approximation. The model problem is

$$2in_0k_0\partial_z u = \partial_x^2 u + (n^2 - n_0^2)k_0^2 u$$

with

$$k_0 = 2\pi/\lambda, \quad \lambda = 0.832, \quad n = 1,$$

with the initial condition and the reference index n_0 in the first case

Example 1

$$\begin{cases} u(x, z=0) = \exp(-(x/10)^2)\exp(-in_0\sin(\alpha)x) \\ n_0 = \cos(\alpha), \quad \alpha = 21.8^\circ, \end{cases}$$

and in the second case,

Example 2

$$\begin{cases} u(x, z=0) = \Sigma_{j=1,2}\exp(-((x-l_j)/10)^2)\exp(-in_0\sin(\alpha_j)x) \\ l_1 = -12.5, \quad l_2 = 12.5, \quad \alpha_1 = 26.8^\circ, \quad \alpha_2 = 16.8^\circ, \\ n_0 = \cos(\beta), \quad \beta = 21.8^\circ. \end{cases}$$

The first of these involves a single beam with a Gaussian profile propagating in vacuum, $n = 1$, at a wavelength of 0.832 μm and describing an angle of $\alpha = 21.8^\circ$ with respect to the z-axis. The computational window has a width of 200 μm and the propagation step length $\Delta z = 0.4$ μm. The propagation distance of $Z = 500$ μm is selected to yield a single reflection from the boundary.The second set of comparisons involves a superposition of two Gaussian beams, one placed at a distance -12.5 μm from the coordinate origin and propagating at an angle of 26.8° and the second placed at $+12.5$ μm from the coordinate origin and propagating at 16.8°. In all test cases a uniform finite-difference discretization in x-direction has been utilized together with the implicit midpoint rule in the direction of propagation (z-axis). In order to visualize the residual reflections the 10^{-10}, 10^{-8}, 10^{-6}, 10^{-4}, 10^{-2}, 10^{-1} iso-lines of $|u(x, z)|^2$, where $u(x, z)$ is the numerically calculated electric field profile normalized with respect to the discrete L^2-norm such that $\|u(x, 0)\| = 1$, are plotted.

Semidiscrete Approach. Figure 1 displays the iso-line plot for the first test case corresponding to the propagation of a single beam on a uniform $N = 1024$ point transverse grid. As expected from the above theory, some small reflections are produced by the discretization error in the transverse, x, direction. Our simulation of the second test example in Fig. 2 supplies similar results. The magnitude of the reflections are approximately the same as in the former case despite the far more complicated shape of the field at the window boundaries.

In order to verify that the magnitude of the reflection depends on the accuracy of the inner solution rather than on the shape of the propagating field, we have repeated our numerical experiments for $N = 8192$ transverse discret-

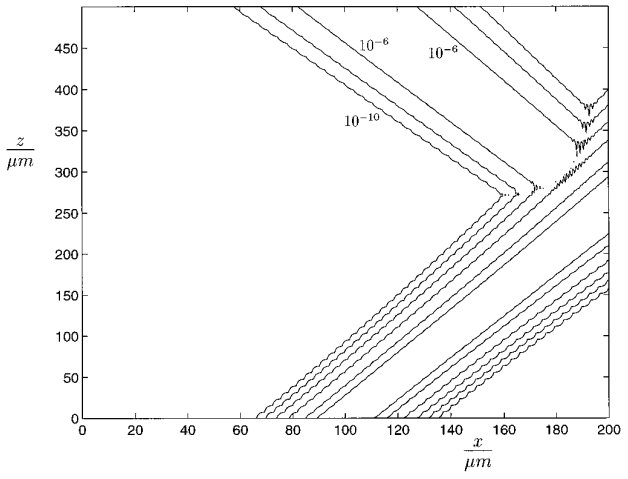

FIG. 1. Iso-curves for the electric power for a single Gaussian beam and $N = 1024$ grid points.

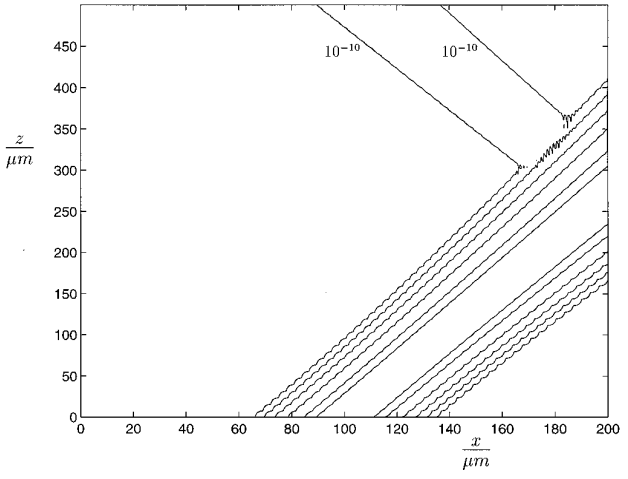

FIG. 3. Iso power curves for the single-beam test case with $N = 8192$.

ization points, generating the results given in Fig. 3 and Fig. 4. It is evident from these figures that the spurious reflections are suppressed as the accuracy of the inner solution increases.

In Fig. 5, we instead present the discrete L^2-norm of the field, $u(x, z)$, remaining inside the computational window as a function of the number of transverse discretization points. The plateaus in the figures indicate the power reflection coefficient after an integer number of reflections. Clearly, these results confirm that magnitude of the reflection coefficient varies with the x-discretization error of the problem in the interior domain.

We finally demonstrate that the spurious reflections of the previous examples can be avoided with the aid of our full discrete approach, for uniformly spaced grid points. Repeating our test examples with $N = 1024$ grid points, we thus obtain the iso-lines of Figs. 6 and 7 which contain no observable reflected power. The corresponding evolution of the discrete L^2-norm is presented in Fig. 8 over a distance of 500 μm, which equates to 1250 propagation steps. The full discrete approach is here numerically preferable, as is expected to be generally true for uniform meshes although, as noted above, the method assumes a continuation of the uniform mesh throughout the exterior domain. To verify the stability of our algorithm subject to finite computer arithmetics, we have repeated this calculation for 10,000 propagation steps. The resulting discrete L^2-

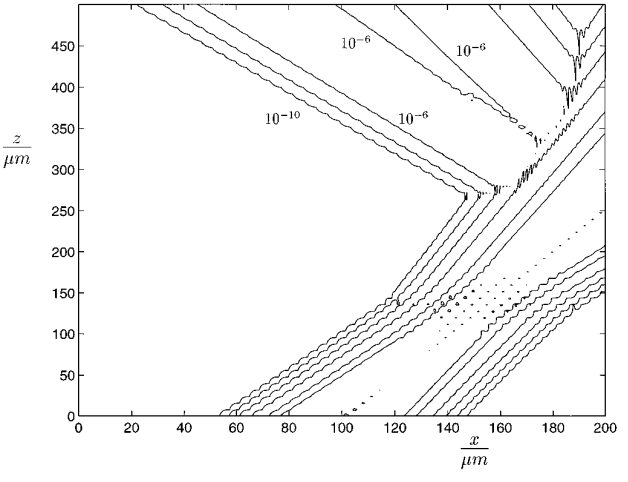

FIG. 2. Iso power curves for a two-beam test case with $N = 1024$.

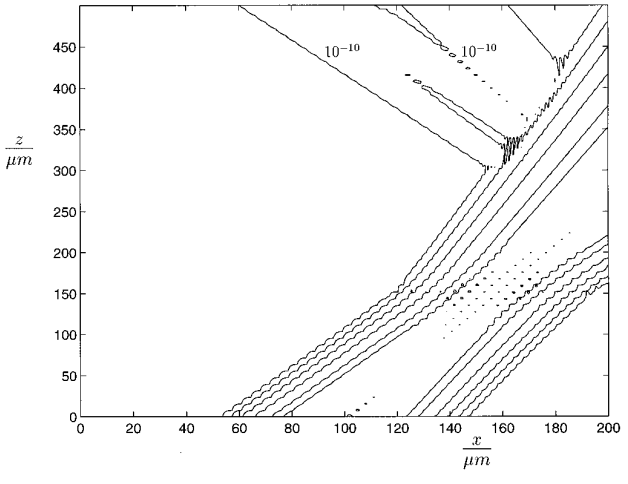

FIG. 4. Iso power curves for the two-beam case with $N = 8192$.

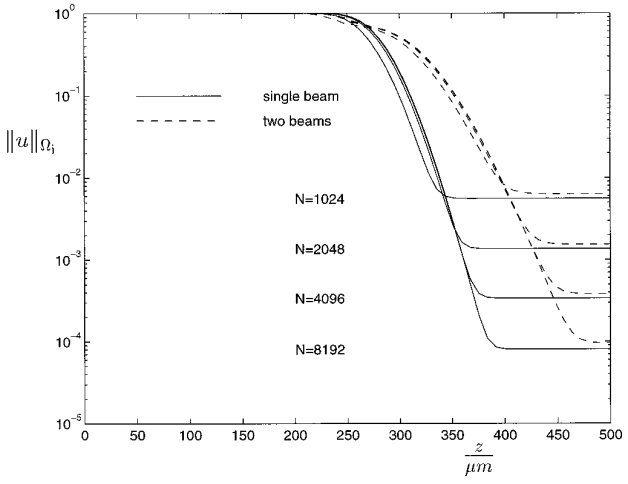

FIG. 5. The discrete L^2-norm of the electric field remaining inside the computational window for $N = 8192$.

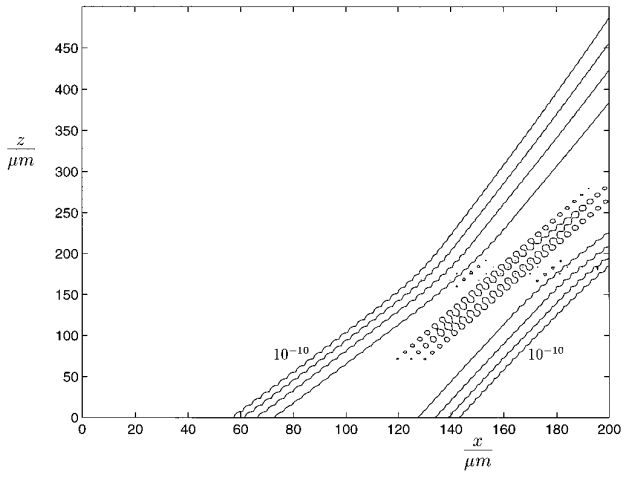

FIG. 7. Iso-curves for the two-beam test case with $N = 1024$ in the full discrete approach.

norm of the field remaining inside the computational window, which evolves as shown in Fig. 9, then decreases approximately to 10^{-12}. This figure is in good accordance with the product of the 10^3 nodes with the 10^{-15} machine accuracy and clearly demonstrates the stability of our algorithm.

CONCLUSIONS

We have constructed general transparent boundary conditions for uniformly discretized 1D Schrödinger-type equations based on a recursive semi-discrete formulation presented in [11]. As our method is derived directly from the Mikusiński' operator theory, Z-transforms in the time variable of the field at the boundary are not present. Accordingly, our derivatives and formulas are particularly simple in nature, yielding additional insight into the structure and behavior of reflectionless boundary conditions.

APPENDIX A: TAYLOR SERIES EXPANSION OF THE SQUARE ROOTS INVOLVING THE SHIFT-OPERATOR

The central enabling feature of our technique is the approximation of square-root operators such as $\sqrt{1-s}$ involving the shift-operator s by a finite number of Taylor

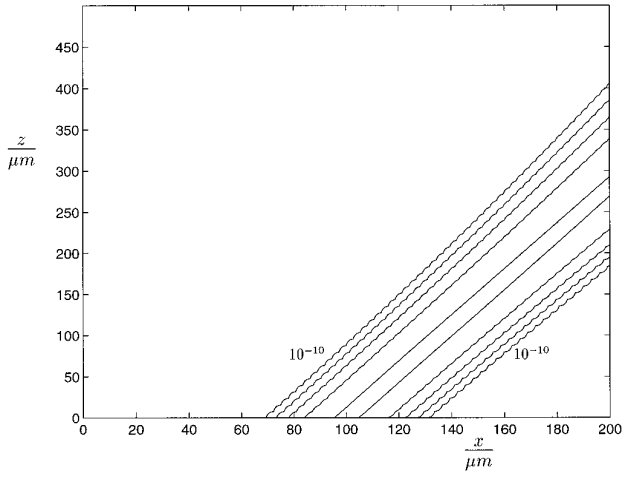

FIG. 6. Iso power curves for the single-beam with $N = 1024$ in the full discrete approach.

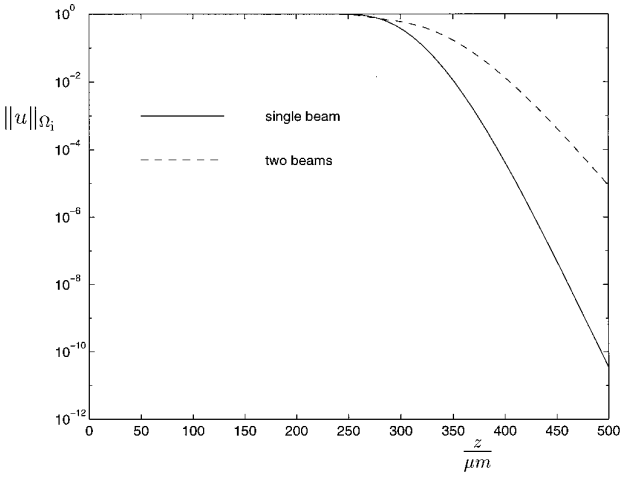

FIG. 8. Discrete L^2-norm of the electric field remaining inside the computational window for $N = 1024$.

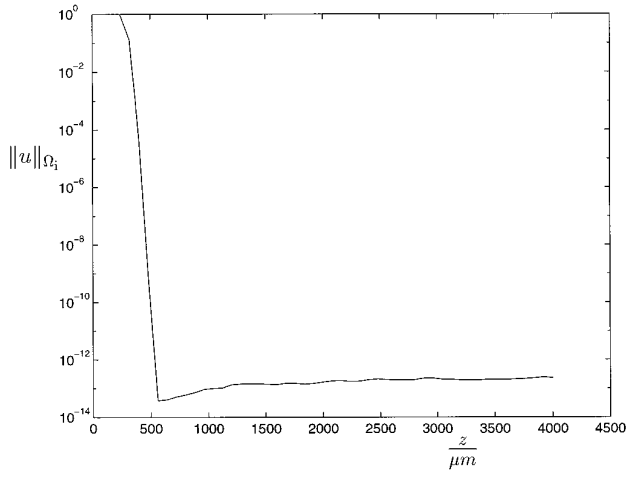

FIG. 9. Discrete L^2-norm of the electric field remaining inside the computational window for $N = 1024$ and 10,000 propagation steps (example 1). The solution-process remains stable.

series terms. A mathematical justification of the expansion is provided through the algebraic operator theory of Mikusiński [10]. A greatly simplified framework can, however, be developed in our special case leading to the alternative, compact justification presented below. Although our considerations may be easily adapted to the general case, we here simplify our discussion to the semi-discrete formalism and further set $\theta = 1$, corresponding to the implicit Euler discretization.

After the ith propagation step, $i \geq 1$, the sequence of boundary values $\{u_0(0), u_1(0), ..., u_i(0)\}$, as well as the sequence of the Laplace-transformed exterior solutions $\{U_0(p), U_1(p), ..., U_i(p)\}$, are determined, where by definition $u_0(0) = 0$ and $U_0(p) = 0$. Let us extend these sequences to $\{..., u_{-1}(0), u_0(0), ..., u_i(0)\}$ and $\{..., U_{-1}(p), U_0(p), ..., U_i(p)\}$ with $u_j(0) = 0$ and $U_j(p) = 0$ for $j \leq 0$. At step $i + 1$ it holds (see (12)) that

$$(p^2 - \lambda^2(1 - s))\, U_{i+1}(p) = p u_{i+1}(0) + \partial_x u_{i+1}|_{x=0}. \quad (32)$$

We want to factor $p^2 - \lambda^2(1 + s)$ in the above expression according to

$$\left(p - \sum_{j=0}^{i} \alpha_j s^j\right)\left(p - \sum_{j=0}^{i} \beta_j s^j\right) U_{i+1}(p) = (p^2 - \lambda^2(1 - s))\, U_{i+1}(p), \quad \alpha_j, \beta_j \in \mathbf{C}.$$

To this end we introduce the notation

$$[\sqrt{1 + a}]_i = 1 + \sum_{j=1}^{i} \binom{1/2}{j} a^j,$$

to represent the order i Taylor series expansion of $\sqrt{1 + a}$, $a \in \mathbf{C}$, at $a = 0$. That is, $[\sqrt{1 + a}]_i - \sqrt{1 + a} = O(a^{i+1})$, in which we select the branch of the square root with $\Re(\sqrt{1 + a}) > 0$. Clearly, we have for any $a \in \mathbf{C}$, $\Re(\lambda) > 0$,

$$(p^2 - \lambda^2(1 + a)) = (p + \lambda[\sqrt{1 + a}]_i)\,(p - \lambda[\sqrt{1 + a}]_i) + O(a^{i+1}).$$

Here we can replace the complex number a by the operator $-s$. Now (32) transforms into

$$(p - \lambda[\sqrt{1 - s}]_i)(p + \lambda[\sqrt{1 - s}]_i) u_{i+1}(p) = p u_{i+1}(0) + \partial_x u_{i+1}|_{x=0}, \quad (33)$$

because the term $O(s^{i+1}) U_{i+1}(p)$ is identically zero. Our discrete transparent boundary condition (15), $\partial_x u_{i+1}|_{x=0} + \lambda[\sqrt{1 - s}]_i u_{i+1}(0) = 0$, inserted into (33) finally yields

$$(p - \lambda[\sqrt{1 - s}]_i)((p + \lambda[\sqrt{1 - s}]_i) U_{i+1}(p) - u_{i+1}(0)) = 0. \quad (34)$$

We now establish that a solution $U_{i+1}(p)$ of (34) does not contain poles with $\Re(p) > 0$ if such poles do not appear in any $U_j(p)$ $1 \leq j \leq i$. Recasting (34) into the form

$$(p + \lambda) U_{i+1}(p) = \lambda(1 - [\sqrt{1 - s}]_i) U_{i+1}(p) + u_{i+1}(0) = -\lambda \sum_{j=1}^{i} (-1)^j \binom{1/2}{j} U_{i-j+1}(p) + u_{i+1}(0)$$

shows that the additional pole generated at the $(i + 1)$th recurrence step appears at $p = -\lambda$. The analyticity of $U_{i+1}(p)$ for all $\Re(p) > 0$ is thus assured if any $U_j(p)$, $1 \leq j \leq i$ is analytic in the same domain.

ACKNOWLEDGMENTS

The authors acknowledge the continuous support and helpful discussions by P. Deuflhard and F. A. Bornemann. One of us (D.Y.) would like to acknowledge support from the Ontario Centre for Materials Research, Bell Northern Research, Corning Glass, and the National Sciences and Research Council of Canada. Finally we want to thank the reviewers for their helpful comments.

REFERENCES

1. A. Arnold, Numerically absorbing boundary conditions for quantum evolution equations, Preprint No. 481, Department of Mathematics, Technical University, Berlin, 1995 (unpublished).
2. V. A. Baskakov and A. V. Popov, *Wave Motion* **14,** 123 (1991).
3. E. Eisenberg, Sh. Ron, and M. Baer, *J. Chem. Phys.* **101,** 3802 (1994).
4. B. Engquist and A. Majda, *Math. Comp.* **31,** 629 (1977).
5. L. Halpern, *SIAM J. Math. Anal.* **22,** 1256 (1991).

6. T. M. Hagstrom, *SIAM J. Num. Anal.* **23,** 948 (1986).
7. R. Kosloff and D. Kosloff, *J. Comput. Phys.* **63,** 363 (1986).
8. D. Macías, S. Brouard, and J. G. Muga, *Chem. Phys. Letr.* **228,** 672 (1995).
9. B. Mayfield, *Nonlocal Boundary Condition for the Schrödinger Equation, Ph.D. thesis*, University of Rhode Island, Providence, RI, 1989 (unpublished).
10. J. Mikusiński, *Operatorenrechnung* (Deutscher Verlag der Wissenschaften, Berlin, 1957).
11. F. Schmidt and P. Deuflhard, *Computers Math. Appl.* **29,** 53 (1995).
12. R. Renault and J. Fröhlich, *J. Comput. Phys.* **124,** 324 (1996).
13. Á. Vibók and G. D. Balint-Kurti, *J. Chem. Phys.* **96,** 7615 (1992).
14. D. Yevick, J. Yu, and Y. Yayon, *J. Opt. Soc. Am. A* **12,** 107 (1995).